ISSN: 0067-2904

Theoretical Study of Elastic Electron Scattering from ^{8}B, ^{17}Ne, ^{11}Be and ^{11}Li Halo Nuclei

Arkan R. Ridha*, Wasan Z. Majeed
Department of physics, College of science, University of Baghdad, Baghdad, Iraq

Received: 17/6/2019 Accepted: 17/4/2021

Abstract

The nuclear density distributions and size radii are calculated for one-proton ^{8}B, two-proton ^{17}Ne, one-neutron ^{11}Be and two-neutron ^{11}Li halo nuclei. The theoretical outlines of calculations assume that the nuclei understudy are composed of two parts: the stable core and the unstable halo. The core part is studied using the radial wave functions of harmonic-oscillator (HO) potentials, while the halo is studied through Woods-Saxon (WS) potential. The long tail behaviour which is the main characteristic of the halo nuclei are well generated in comparison with experimental data. The calculated size radii are in good agreement with experimental values. The elastic electron scattering form factors of the C0 component are also calculated for the aforementioned nuclei. The calculated form factor results give predictions for the results of future experiments on electron-radioactive ion beam colliders.
PACS number(s): 21.10.Gv, 21.60.Cs, 25.30.Bf

Keywords: halo nuclei, nuclear density distributions, elastic electron scattering form factors, root-mean square radii, Woods-Saxon potential.

دراسة نظرية للأستطارة الألكترونية المرنة من النوى الهالة ^{8}B و ^{17}Ne و ^{11}Be و ^{11}Li

اركان رفعه رضا* و وسن زهير مجيد
قسم الفيزياء، كلية العلوم، جامعة بغداد، بغداد,العراق

الخلاصة

تم حساب توزيعات الكثافة وانصاف الاقطار النووية للنوى الهالة ذو البروتون الواحد بورون- 8 وذو البروتونين نيون- 17 وذو النيوترون الواحد بيريليوم- 11 وذو النيوترونين ليثيوم- 11. الخطوط العامة النظرية للحسابات تفرض ان الانوية تحت الدراسة هي مكونة من جزئين: الاول يمثل القلب المستقر والثاني جزء الهالة غير المستقر. القلب تم دراسته باستخدام الدوال الموجية القطرية لجهد المتذبذب التوافقي البسيط بينما جزء الهالة فتم درسته من خلال الدوال الموجية القطرية لجهد وودز-ساكسون. خاصية التذييل الممتد والذي هو الصفة المميزة للنوى الهالة تم توليدها بصورة جيدة بالمقارنة مع البيانات العملية. انصاف الاقطار المحسوبة كانت مع تطابق جيد مع تلكم العملية. عوامل التشكل للاستطارة الالكترونية المرنة للمركبة C0 ايضا تم حسابها للنوى المذكورة اعلاه. نتائج عوامل التشكل المحسوبة تعطي تنبؤات لنتائج التجارب المستقبلية لصادم الكترون-الحزم المشعة الايونية.

*Email: Arkan.Ridha@sc.uobaghdad.edu.iq

1. Introduction

Electron–nucleus scattering is one of the dominant tools for investigating nuclear charge density distributions. Nuclear size and density distribution are the essential quantities to explain nuclear properties [1]. The development of radioactive isotope beam techniques has opened a new field for the study of unstable nuclei far from the stability line [2] [3]. Therefore, it is very interesting to theoretically study the properties of unstable nuclei according to reliable theories and models.

One and two neutron (proton) halos have now been observed in several light neutron-rich nuclei, such as ^{8}B, ^{11}Be, ^{17}Ne and ^{11}Li. Minamisono et al. [4] succeeded in a precise measurement of the quadrupole moment of ^{8}B. They pointed out that the quadrupole moment of ^{8}B is considerably larger than the shell-model prediction.

Zukov and Thompson [5] studied the proton drip-line nucleus ^{17}Ne in a three-body model of ^{15}O plus two protons. The model gives a proton radius larger by about 0.26-0.32 fm than the neutron radius, showing that a proton skin is present.

Al- Khalili et al., [6] explored the root mean square matter radii of halo ^{11}Be, ^{6}He, ^{11}Li and ^{14}Be nuclei from the measured reaction cross sections at high energy using a Glauber type calculation.

The ^{8}B nucleus has been investigated using two frequency shell model approach by Majeed [7], where the configuration mixing shell- model was carried out using a model space for the core nucleus different from that for proton halo. This assumption was supported by the fact that the valence proton was distributed in a spatial region which is much larger than the core.

The aim of the present work is to study nuclear densities, *rms* radii and elastic electron scattering form factors of halo ^{8}B, ^{17}Ne, ^{11}Be and ^{11}Li nuclei. The radial wave functions of harmonic-oscillator (HO) and Woods-Saxon (WS) potentials are used to calculate the afore mentioned quantities for core and halo parts, respectively.

2. Theoretical Formulations

The ground density distributions of point neutron and proton of halo nuclei can be written as [8]:

$$\rho_{t_z}(r) = \rho^{c}_{t_z}(r) + \rho^{h}_{t_z}(r) \tag{1}$$

where $t_z = \frac{1}{2}$ for protons or $t_z = -\frac{1}{2}$ for neutrons. $\rho^{c}_{t_z}(r)$ is calculated through harmonic-oscillator (HO) radial wave functions ($R_{nl}(r)$) [9] and can be written as [8]:

$$\rho^{c}_{t_z}(r) = \frac{1}{4\pi}\sum_{nl} N^{nl,core}_{t_z} \left|R_{nl}(r, b_{t_z})\right|^2 \tag{2}$$

$N^{nl,core}_{t_z}$ represents the number of neutrons or protons in the nl shell, n and l represent the principal and orbital quantum numbers, respectively. It is worth mentioning that the summation in Eq. (2) spans all occupied orbits in the core for any nuclear sample under study. $\rho^{h}_{t_z}(r)$ in Eq. (1) represents the density distribution for halo part and it is calculated through Woods-Saxon (WS) radial wave functions and can be written as [8]:

$$\rho^{h}_{n,p,m}(r) = \frac{1}{4\pi} N^{nlj,halo}_{t_z} \left|R_{nlj,t_z}(r)\right|^2 \tag{3}$$

where $N^{nlj,halo}_{t_z}$ represents the number of neutrons or protons in the sub-shell nlj, j represents the total angular quantum number. The $R_{nlj,t_z}(r)$ in Eq. (3) is the solution to the radial of Schrödinger equation [10]:

$$\left(\frac{\hbar^2}{2\mu}\frac{d^2}{dr^2} - v(r) - \frac{l(l+1)\hbar^2}{2\mu r^2} + \varepsilon_{nlj,t_z}\right) R_{nlj,t_z}(r) = 0 \tag{4}$$

where $\mu = m_n(A-1)/A$ is the reduced mass of the core $(A-1)$ and single nucleon, m_n is the nucleon mass, A is the atomic mass, ε_{nlj} is the single halo nucleon separation energy.
For the local potential $v(r)$, the WS shape is used in the compact form as shown below [11] [12]:

$$v(r) = v_{cent}(r) + v_{s.o.}(r) + v_c(r) \quad (5)$$

where

$$v_{cent}(r) = \frac{-U_0}{\left(1+e^{\left(\frac{r-R}{a}\right)}\right)} \quad (6)$$

represents the central part of $v(r)$, U_0 is the strength or depth of central potential, a_0 is the diffuseness and $R = r_0(A-1)^{1/3}$ is the radius parameter of the central potential.

$$v_{s.o.}(r) = \left(\frac{\hbar}{m_\pi c}\right)^2 \frac{U_{s.o.}}{r}\frac{d}{dr}\frac{1}{\left(1+e^{\left(\frac{1-R_{s.o.}}{a_{s.o.}}\right)}\right)}\langle \hat{l}.\hat{\sigma}\rangle = -\left(\frac{\hbar}{m_\pi c}\right)^2 \frac{U_{s.o.}}{r a_{s.o.}}\frac{e^{\left(\frac{r-R_{s.o.}}{a_{s.o.}}\right)}}{\left(1+e^{\left(\frac{r-R_{s.o.}}{a_{s.o.}}\right)}\right)^2}\langle \hat{l}.\hat{\sigma}\rangle \quad (7)$$

where $\left(\frac{\hbar c}{m_\pi c^2}\right)^2 \approx 2\ fm^2$, $m_\pi c^2 = 139.567\ MeV$ and $\hbar c = 197.329\ MeV fm^2$.

$$\langle \hat{l}.\hat{\sigma}\rangle = \begin{cases} -\frac{1}{2}(l+1) & for\ j = l - \frac{1}{2} \\ \frac{1}{2}l & for\ j = l + \frac{1}{2} \end{cases}$$

Eq. (7) represents the spin-orbit part of $v(r)$, m_π is the pion mass, $U_{s.o.}$ is the strength or depth of spin-orbit potential, $a_{s.o.}$ is the diffuseness of spin-orbit part, $R_{s.o.} = r_{s.o.}(A-1)^{1/3}$ is the radius parameter of spin-orbit and $\hat{l}$ and $\hat{\sigma}$ are the angular momentum and the spin operators, respectively.
Finally, in Eq. (5), $v_c(r)$ indicates the Coulomb potential generated by a homogeneous charged sphere and can be written for protons as [13]:

$$v_C(r) = \begin{cases} (Z-1)\frac{e^2}{r} & if\ r > R_C \\ \frac{(Z-1)e^2}{2R}\left[3 - \frac{r^2}{R^2}\right] & if\ r < R_C \end{cases}, \quad (8)$$

and $v_C(r) = 0$ for neutrons, with $e^2 = 1.44\ MeV.fm$. R_C is Coulomb radius of the nucleus and is usually taken to be equal to R.
Therefore, Eq. (5) can be written as:

$$v(r) = \frac{-U_0}{\left(1+e^{\left(\frac{r-R}{a}\right)}\right)} - \left(\frac{\hbar}{m_\pi c}\right)^2 \frac{1}{r}\frac{U_{s.o.}}{a_{s.o.}}\frac{e^{\left(\frac{r-R_{s.o.}}{a_{s.o.}}\right)}}{\left(1+e^{\left(\frac{r-R_{s.o.}}{a_{s.o.}}\right)}\right)^2}\langle \hat{l}.\hat{\sigma}\rangle + v_C(r) \quad (9)$$

In order to compare the calculated point proton density distributions with the experimental densities, the finite proton size is required to be included. The charge density distribution $\rho_{ch}(r)$ (CDD) is obtained by folding the proton density ρ_{pr} into the distribution of the point proton density in Eq. (1) as follows [11]:

$$\rho_{ch}(r) = \int \rho_p(r)\rho_{pr}(\boldsymbol{r} - \boldsymbol{r'})d\boldsymbol{r'} \quad (10)$$

If $\rho_p(\vec{r})$ is taken to have a Gaussian form, then

$$\rho_{pr}(r) = \frac{1}{\left(\sqrt{\pi}a_{pr}\right)^3} e^{\left(\frac{-r^2}{a_{pr}^2}\right)} \quad (11)$$

where $a_{pr} = 0.65\ fm$. Such value of a_{pr} reproduces the experimental charge rms radius of the proton, $\langle r^2 \rangle_{pr}^{1/2} = \left(\frac{3}{2}\right)^{1/2} a_{pr} \approx 0.8\ fm$.

The ground matter density distributions (MDD) of halo nuclei are calculated from:

$$\rho_m(r) = \rho_{t_z=p}(r) + \rho_{t_z=n}(r) \tag{12}$$

The rms radii of neutron, proton, charge and matter can be directly deduced from their density distributions [11] as follows:

$$\langle r^2 \rangle_g^{1/2} = \sqrt{\frac{4\pi}{g} \int_0^\infty \rho_g(r) r^2 dr} \tag{13}$$

g in Eq. (13) denotes to N (number of neutrons), Z (atomic number which is the same for proton and charge) and A, respectively.

The longitudinal electron scattering form factors in the first Born approximation can be calculated from [14] [15]:

$$\left|F_J^C(q)\right|^2 = \frac{4\pi}{Z^2(2J_i+1)} \left|\langle J_f \| \boldsymbol{O}_J^C(q) \| J_i \rangle\right|^2 \tag{14}$$

where q represents the momentum transfer from electron to nucleus during scattering. Eq. (14) can be simplified more to [16]:

$$\left|F_J^C(q)\right|^2 = \frac{4\pi}{Z^2(2J_i+1)} \left|\int_0^\infty j_J(qr)\, \rho_J(r) r^2 dr\right|^2 \tag{15}$$

$j_J(qr)$ and $\rho_J(r)$ are spherical Bessel function and transition density distribution, respectively. For $q = 0$, the electron scattering charge form factor can be written as:

$$|F_{ch}(q)|^2 = \frac{4\pi}{Z^2(2J_i+1)} \left|\int_0^\infty j_0(qr)\, \rho_{ch}(r) r^2 dr\right|^2 \tag{16}$$

3. Results and discussion

The technique of calculation is based on dividing the nuclear system under study into two parts: the first is the stable core which is studied using the radial wave functions of HO potential and the second part is the unstable halo part which is studied using the radial wave function of WS potential. The calculations in such method are denoted by HO+WS. In the core part, two HO size parameters were used: one for protons (b_p) and the second for neutrons (b_n) in order to regenerate the experimental rms radii.

The parameters of WS potential (U_0, $U_{s.o.}$, a_0, $a_{s.o.}$, r_0, $r_{s.o.}$, and R_C) were chosen so as to regenerate the experimental single-nucleon separation energies [17] of the one-halo nuclei or $s_{n(p)} = s_{2n(2p)}/2$ of the two-nucleon halo nuclei.

For ^{8}B, ^{17}Ne, ^{11}Be and ^{11}Li nuclei, the chosen HO size parameters for protons and neutrons for core part and parameters for the WS potential for halo are presented in Table 1.

The calculated rms proton, charge, neutron, and matter radii are presented in Table 2. The calculated results of the rms charge and matter radii are well predicted for the four nuclei under study.

The calculated MDDs are shown in Figure 1(a) for ^{8}B, 1(b) for ^{17}Ne, 1(c) for ^{11}Be, and 1(d) for ^{11}Li and are compared with the experimental data (ref. [18] for ^{8}B, ref. [19], for ^{17}Ne, ref. [20] for ^{11}Be and ref. [21] for ^{11}Li). The dashed and dashed-dotted curves represent the calculated MDDs for core and halo parts in HO and WS radial wave functions, respectively. The solid curves represent total MDDs (core+halo). Excellent agreements with experimental MDDs are obtained for all cases in Figure 1.

The calculated neutron and proton density distributions are presented in Figure 2(a)for ^{8}B, 2(b) for ^{17}Ne, 2(c) for ^{11}Be, and 2(d) for ^{11}Li. The solid and dashed lines are for the calculated neutron and proton density distributions, respectively. The long tail of the proton density curves of one-proton ^{8}B and two-proton ^{17}Ne halo nuclei is clearly observed and investigated,

besides, the long tail of the neutron density curves of one-neutron ^{11}Be and two-neutron ^{11}Li halo nuclei is clearly generated.

In Figure 3, the logarithm ratios of proton over neutron density distributions (for proton halo ^{8}B, Figure 3(a), and ^{17}Ne, Figure 3(b), nuclei) and of neutron over proton density distributions (for neutron halo ^{11}Be, Figure 3(c), and ^{11}Li, Figure 3(d), nuclei) are presented. It is clear from these curves that there was dramatic increase in the logarithm ratios indicating and confirming the halo structure in the nuclei under study.

The results of the calculated elastic electron scattering charge form factors are illustrated in Figure 4(a) for ^{8}B, 4(b) for ^{17}Ne, 4(c) for ^{11}Be, and 4(d) for ^{11}Li and are compared with experimental data of the corresponding stable ^{10}B, ^{20}Ne, ^{9}Be and ^{7}Li nuclei (refs. [22] [23] for ^{10}B, ref. [24] for ^{20}Ne, refs. [25] [26], ref. [27] for ^{9}Be and refs. [28] [29] for ^{7}Li). The solid curves represent the calculated charge form factor in HO+WS. The results in Figure 4 give predictions for the future experiments on the electron-radioactive beam colliders where the effect of the neutron and proton halo or skin on the charge density distributions and charge form factors is planned to be studied.

Table 1-HO and WS parameters for core and halo parts

$^{A}_{Z}X_{N}$	HO size paramrters for core (fm)	WO parameters for halo					
		nl_j	$U_0(MeV)$	$U_{s.o.}(MeV)$	$a_0 = a_{s.o.}$ (fm)	$r_0 = r_{s.o.} = R_C$ (fm)	Separation energy of halo nucleon(s) (MeV) [17]
$^{8}_{5}B_3$	$b_n = 1.514$ $b_p = 1.641$	$1p_{1/2}$	63.13	10.	0.6	1.2	$s_p = 0.13639 \pm 0.001$
$^{17}_{10}Ne_7$	$b_n = 1.594$ $b_p = 1.600$	$2s_{1/2}$	59.966	10.	0.6	1.2	$s_{2p} = 0.9331 \pm 0.00061$
$^{11}_{4}Be_7$	$b_n = 1.638$ $b_p = 1.637$	$2s_{1/2}$	62.52	10.	0.6	1.2	$s_n = 0.50164 \pm 0.00025$
$^{11}_{3}Li_8$	$b_n = 1.750$ $b_p = 1.737$	$1p_{1/2}$	44.78	10.	0.6	1.2	$s_{2n} = 0.36928 \pm 0.00064$

Table 2-Calculated and experimental *rms* charge, proton, neutron and matter radii

nucleus	$\langle r_{ch}^2\rangle_{Cal}^{1/2}$ (fm)	$\langle r_{ch}^2\rangle_{Exp}^{1/2}$ (fm)	$\langle r_p^2\rangle_{Cal}^{1/2}$ (fm)	$\langle r_n^2\rangle_{Cal}^{1/2}$ (fm)	$\langle r_m^2\rangle_{Cal}^{1/2}$ (fm)	$\langle r_m^2\rangle_{Exp}^{1/2}$ (fm)
$^{8}_{5}B_3$	2.82	2.82 ± 0.06 [30]	2.808	2.05	2.55	2.55 ± 0.08 [31]
$^{17}_{10}Ne_7$	3.045	3.0413 [32]	2.987	2.372	2.750	2.750 ± 0.07 [33]
$^{11}_{4}Be_7$	2.448	2.463 ± 0.016 [34]	2.315	3.456	3.09	3.039 ± 0.038 [33]
$^{11}_{3}Li_8$	2.482	2.482 [32]	2.351	3.671	3.363	$3.34^{+0.04}_{-0.08}$ [35]

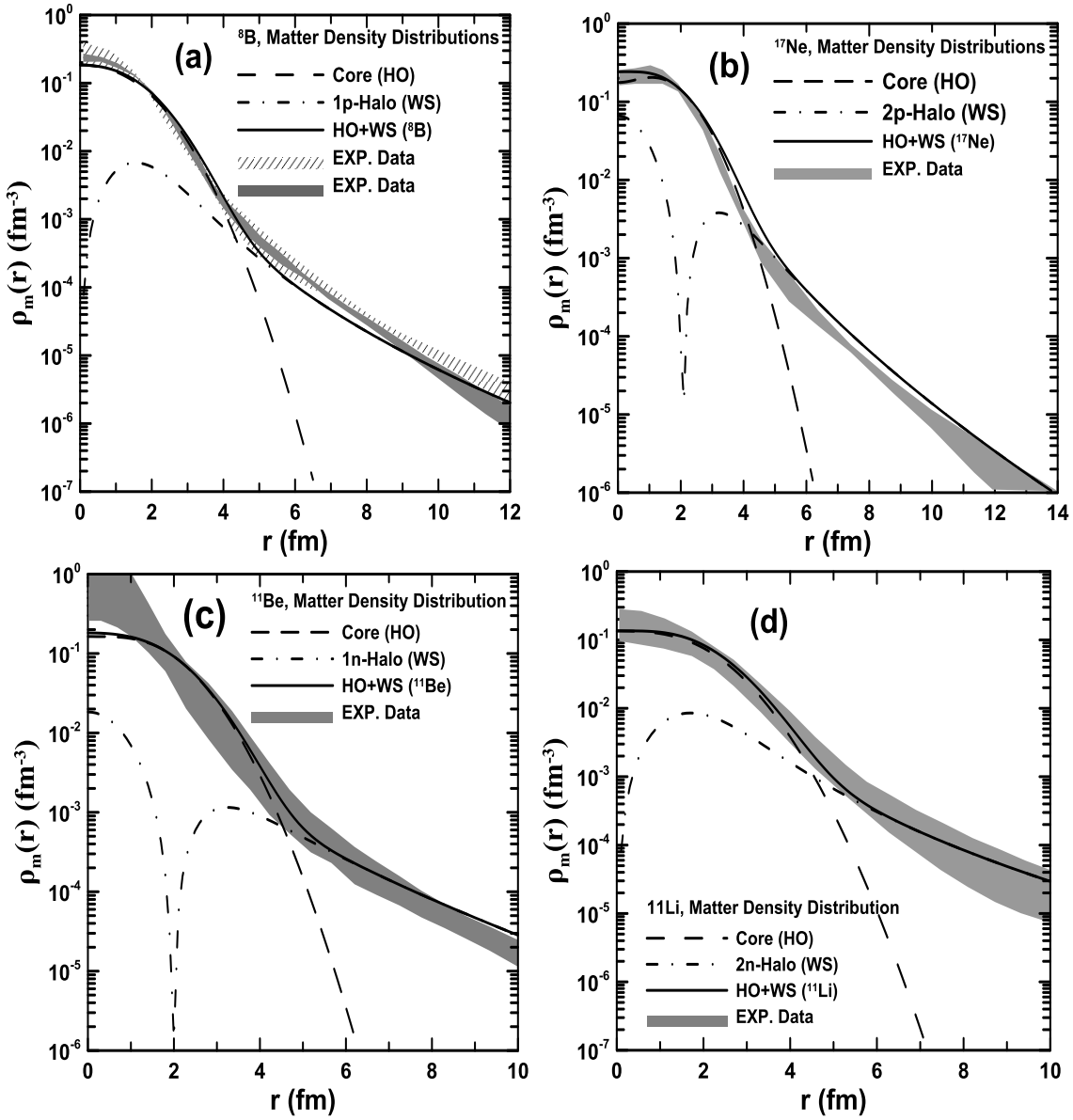

Figure 1-The calculated matter density distributions of the core, halo and total for ^{8}B, ^{17}Ne, ^{11}Be, and ^{11}Li halo nuclei. The experimental data represented by hatched and shaded area in (a) is taken from [18]. The experimental shaded area for ^{17}Ne, ^{11}Be, and ^{11}Li are taken from [19], [20], and [21], respectively.

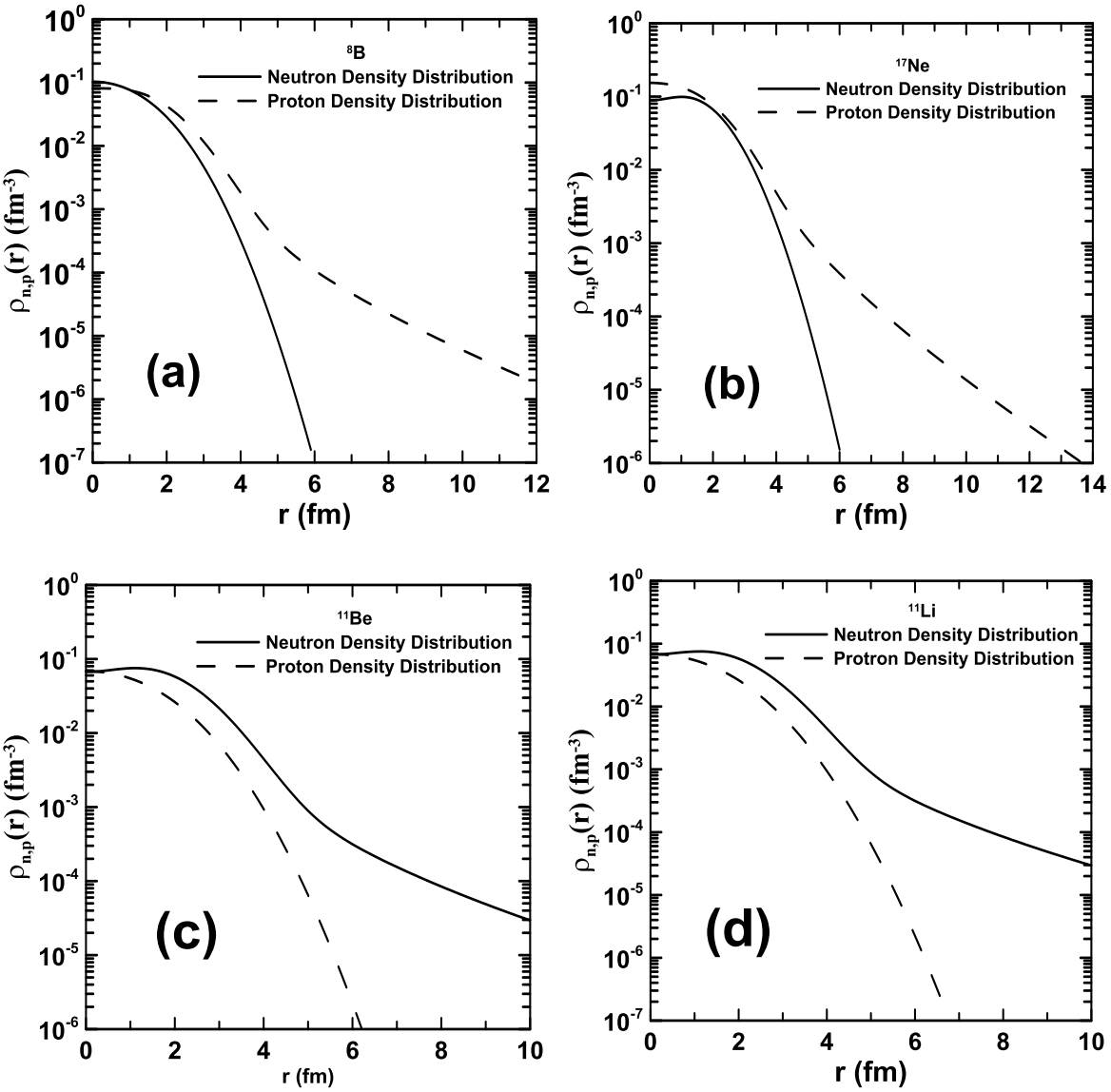

Figure 2-The calculated neutron and proton density distributions of :(a) ^{8}B, (b)^{17}Ne, (c)^{11}Be, and (d) ^{11}Li halo nuclei.

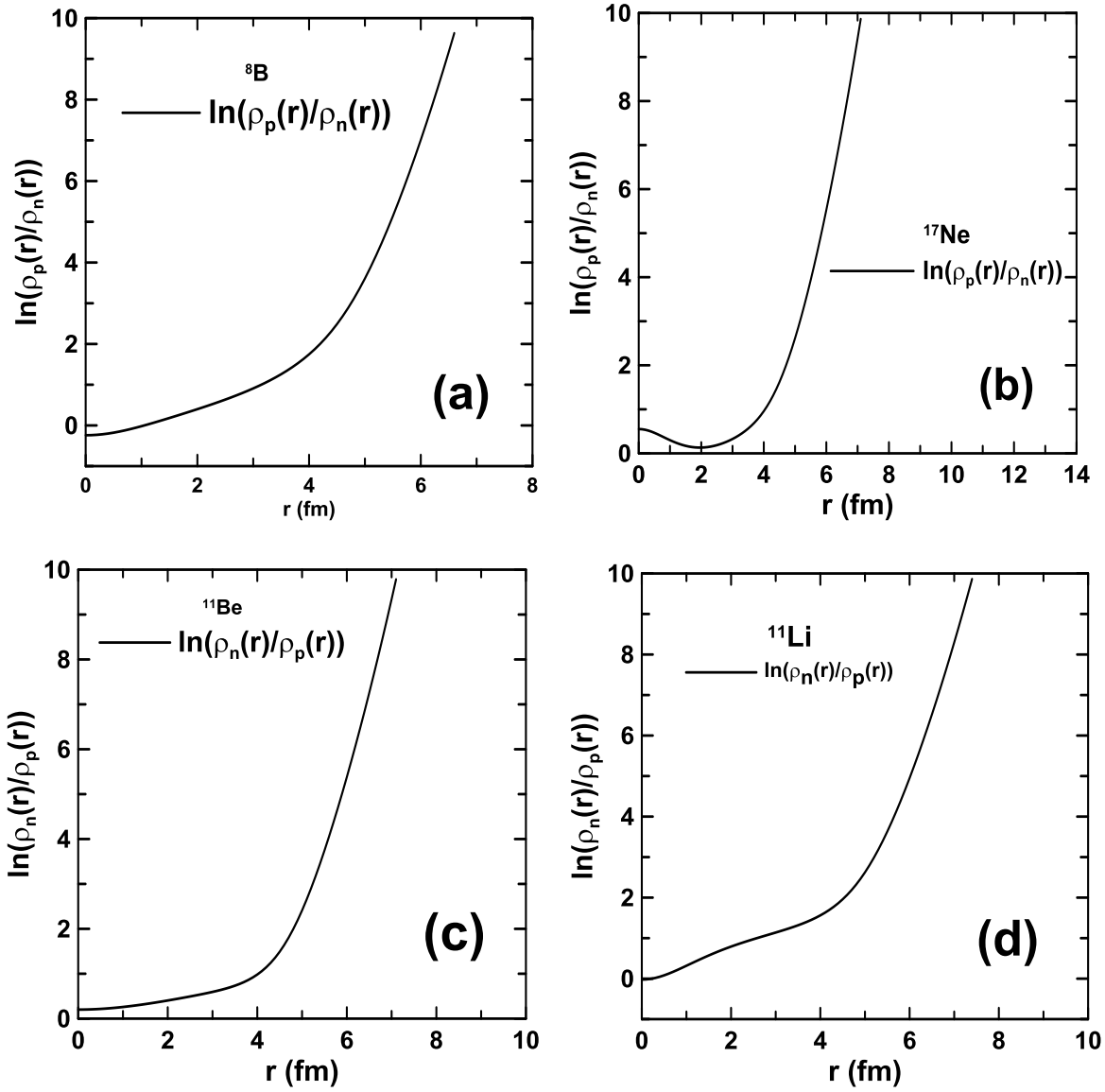

Figure 3-The logarithm ratio of proton over neutron density distributions of proton halo nuclei in ^{8}B (a) and ^{17}Ne (b) and neutron over proton density distributions of neutron halo nuclei in ^{11}Be (c) and ^{11}Li (d).

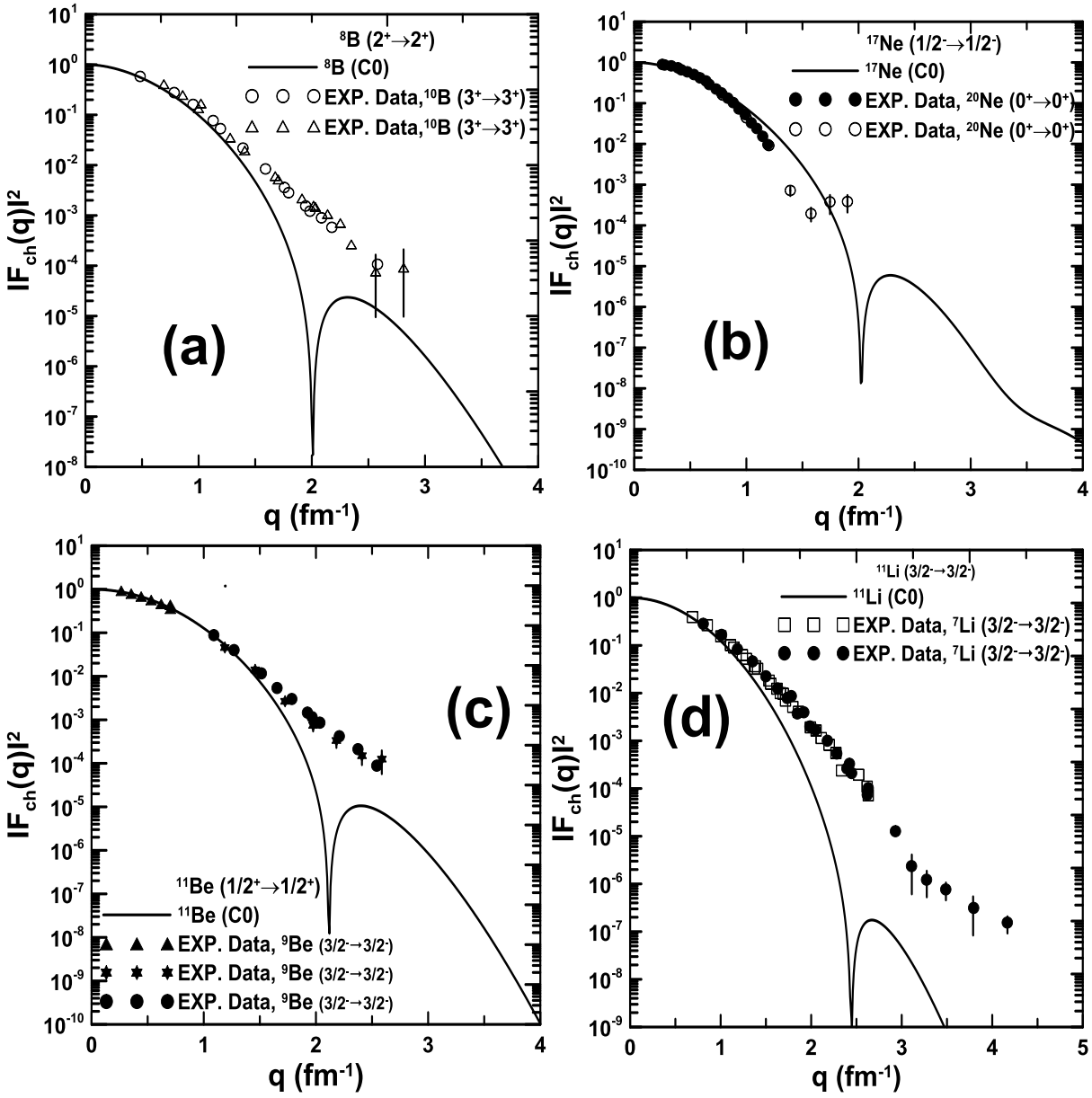

Figure 4-The longitudinal elastic scattering form factors for halo ^{8}B, ^{17}Ne, ^{11}Be, and ^{11}Li nuclei compared with stable ^{10}B, ^{20}Ne, ^{9}Be, and ^{7}Li nuclei. The experimental data for ^{10}B are represented by empty circles [22] and triangles [23]. The experimental data for ^{20}Ne represented by empty and filled circles are taken from [24]. For ^{9}Be, the experimental data are represented by filled circles [25], triangles [26] and stars [27]. Finally, for ^{7}Li, the experimental data are represented by open squares [28] and filled circles [29].

4. Conclusions

The nuclear density distributions of protons, neutrons and nucleons and the corresponding *rms* radii of the halo ^{8}B, ^{17}Ne, ^{11}Be and ^{11}Li are calculated. The single-particle wave functions of HO and WS potentials are used to study the stable core and unstable halo parts, respectively for the nuclei under study. The long tail behaviour in the density distributions is well generated. Very good agreements are obtained for the calculated *rms* charge and matter radii in comparison with the available experimental data. The elastic electron scattering form factor of the C0 component are also studied. The results of the calculated elastic charge form

factors for the nuclei under study are controversial till future experiments on the electron-radioactive beam colliders are settled.

5. References

[1] I. Tanihata, "Neutron halo nuclei," *Journal of Physics G: Nuclear and Particle Physics,* pp. 157-198, 1996.

[2] I. Tanihata, "Nuclear structure studies from reaction induced by radioactive nuclear beams," *Progress in Particle and Nuclear Physics,* vol. 35, pp. 505-573, 1995.

[3] A. C. Mueller, "Radioactive beams in France," *Progress in Particle and Nuclear Physics,* vol. 46, no. 1, pp. 359-374, 2001.

[4] T. Minamisono, T. Ohtsubo, I. Minami, S. Fukuda, A. Kitagawa, M. Fukuda, K. Matsuta, Y. Nojiri, S. Takeda, H. Sagawa, and H. Kitagawa, "Proton halo of 8B disclosed by its giant quadrupole moment," *Physical Review Letters,* vol. 69, no. 14, pp. 2058-2061, 1992.

[5] M. V. Zhukov and I. J. Thompson, "Existence of proton halos near the drip line," *Physical Review C,* Vols. 3505-3508, no. 6, p. 52, 1995.

[6] J. S. Al-Khalili, J. A. Tostevin, and I. J. Thompson, "Radii of halo nuclei from cross section measurements," *Physical Review C,* vol. 54, no. 4, pp. 1843-1852, 1996.

[7] R. A. Radhi, A. K. Hamoudi, and W. Z. Majeed, "Density distributions and form factors of the exotic 8B nucleus," *Iraqi Journal of Physics,* vol. 11, no. 20, pp. 25-34, 2013.

[8] A. K. Hamoudi, R. A. Radhi, and A. R. Ridha , "Elastic electron scattering from 17Ne and 27P exotic nuclei," *Iraqi Journal of Physics,* vol. 13, no. 28, pp. 68-81, 2015.

[9] Von P. J. Brussard and P. W. M. Glaudemans, Shell Model Applications in Nuclear Spectroscopy, Amsterdam: North Holland Publishing, 1977.

[10] B. A. Brown, S. E. Massen and P. E. Hodgson, "Proton and neutron density distributions for A=16-58 nuclei," *Journal of Physics G: Nuclear Physics,* vol. 5, no. 12, pp. 1655-1698, 1979.

[11] L. R. B. Elton and A. Swift, "Single-particle potentials and wave functions in the 1p and 2s-1d shells," *Nuclear Physics A,* vol. 94, no. 1, pp. 52-72, 1967.

[12] S. Gamba, G. Ricco, and G. Rottigni, "A phenomenological woods-saxon potential for p-shell nuclei," *Nuclear Physics A,* vol. 213, no. 2, pp. 383-396, 1973.

[13] Peter Ring and Peter Schuck, The Nuclear Many-Body Problem, New York: Springer-Verlag, 1980.

[14] T. de Forest and J. D. Walecka, "Electron scattering and nuclear structure," *Advances in Physics,* vol. 15, no. 57, pp. 1-109, 1966.

[15] B. A. Brown, B. H. Wildenthal, C. F. Williamson, F. N. Rad, S. Kowalski, Hall Crannell, and J. T. O'Brien, "Shell-model analysis of high-resolution data for elastic and inelastic electron scattering on 19F," *Physical Review C,* vol. 32, no. 4, pp. 1127-1156, 1985.

[16] R. A. Radhi, A. K. Hamoudi and Z. A. Salman, "The Calculation of the Charge Density Distributions and the Longitudinal Form Factors of 10B Nucleus by Using the Occupation Numbers of the States," *Iraqi Journal of Physics,* vol. 7, no. 10, pp. 10-18, 2009.

[17] Meng Wang, G. Audi, F. G. Kondev, W. J. Huang, S. Naimi, and Xing Xu, "The Ame2016 atomic mass evaluation*(II). Tables, graphs and references," *Chinese Physics C,* vol. 41, no. 3, pp. 1-442, 2017.

[18] M. Takechi, M. Fukuda, M. Mihara, T. Chinda, T. Matsumasa, H. Matsubara, Y. Nakashima, K. Matsuta, T. Minamisono, R. Koyama, W. Shinosaki, M. Takahashi, A. Takizawa, T. Ohtsubo, T. Suzuki, T. Izumikawa, S. Momota, K. Tanaka, T. Suda, M. Sasaki, S. Sato , "Reaction cross-sections for stable nuclei and nucleon density distribution of proton drip-line nucleus 8B," *European Physical Journal A,* vol. 25(S1), pp. 217-219, 2005.

[19] K. Tanaka, M. Fukuda, M. Mihara, M. Takechi, T. Chinda, T. Sumikama, S. Kudo, K. Matsuta, T. Minamisono, T. Suzuki, T. Ohtubo, T. Izumikawa, S. Momota, T. Yamaguchi, T. Onishi, A. Ozawa, I. Tanihata and Zheng Tao, "Nucleon density distribution of proton drip-line nucleus

17Ne," *European Physical Journal A*, vol. 25(s01), pp. 221-222, 2005.

[20] M. Fukuda, T. Ichihara, N. Inabe, T. Kubo, H. Kumagai, T. Nakagawa, Y. Yano, I. Tanihata, M. Adachi, K. Asahi, M. Kouguchi, M. Ishihara, H. Sagawa, and S. Shimoura, "Neutron halo in 11Be studied via reaction cross sections," *Physics Letters B*, vol. 268, no. 3-4, pp. 339-344, 1991.

[21] P. Egelhof, G. D. Alkhazov, M. N. Andronenko, A. Bauchet, A. V. Dobrovolsky, S. Fritz, G. E. Gavrilov, H. Geissel, C. Gross, A. V. Khanzadeev, G. A. Korolev, G. Kraus, A. A. Lobodenko, G. Münzenberg, M. Mutterer, S. R. Neumaier, T. Schäfer, C. Scheidenber, "Nuclear-matter distributions of halo nuclei from elastic proton scattering in inverse kinematics," *European Physical Journal A*, vol. 15, pp. 27-33, 2002.

[22] A. Cichocki, J. Dubach, R. S. Hicks, G. A. Peterson, C. W. de Jager, H. de Vries, N. Kalantar-Nayestanaki, and T. Sato, "Electron scattering from 10B," *Physical Review C*, vol. 51, no. 5, pp. 2406-2426, 1995.

[23] T. Stovall, J. Goldemberg, and D. B. Isabelle, "Coulomb form factors of 10B and 11B," *Nuclear Physics* , vol. 86, pp. 225-240, 1966.

[24] E. A. Knight, R. P. Singhal, R. G. Arthur and M. W. S. Macauley, "Elastic scattering of electrons from 20,22Ne," *Journal of Physics G: Nuclear Physics*, vol. 7, pp. 1115-1121, 1981.

[25] J. P. Glickman, W. Bertozzi, T. N. Buti, S. Dixit, F. W. Hersman, C. E. Hyde-Wright, M. V. Hynes, R. W. Lourie, B. E. Norum, J. J. Kelly, B. L. Berman, and D. J. Millener, "Electron scattering from 9Be," *Physical Review C*, vol. 43, no. 4, pp. 1740-1757, 1991.

[26] J. A. Jansen, R. Th. Peerdeman, and C. De Vries, "Nuclear charge radii of 12C and 9Be," *Nuclear Physics A*, vol. 188, no. 2, pp. 337-352, 1972.

[27] M. Bernheim, T. Stovall, and D. Vinciguerra, "Electron scattering from 9Be," *Nuclear Physics A*, vol. 97, no. 3, pp. 488-504, 1967.

[28] L. R. Suelzle, M. R. Yearian, and Hall Crannell, "Elastic Electron Scattering from Li6 and Li7," *Physical Review*, vol. 162, pp. 992-1005, 1967.

[29] J. Lichtenstadt, J. Alster, M. A. Moinester, J. Dubach, R. S. Hicks, G. A. Peterson and S. Kowalski, "High momentum transfer longitudinal and transverse form factors of the 7Li ground-state doublet," *Physics Letters B*, vol. 219, no. 4, pp. 394-398, 1989.

[30] B. Blank, C. Marchand, M. S. Pravikoff, T. Baumann, F. Boué, H. Geissel, M. Hellström, N. Iwasa, W. Schwab, K. Sümmerer, and M. Gaic, "Total interaction and proton-removal cross-section measurements for the proton-rich isotopes 7Be, 8B, and 9C," *Nuclear Physics A*, vol. 624, no. 2, pp. 242-256, 1997.

[31] S. S. Chandel, S. K. Dhiman, and R. Shyam, "Structure of 8B and astrophysical S17 factor in Skyrme Hartree-Fock theory," *Physical Review C*, vol. 68, no. 054320, pp. 1-7, 2003.

[32] I. Angeli and K. P. Marinova, "Table of experimental nuclear ground state charge radii: An update," *Atomic Data and Nuclear Data Tables*, vol. 99, no. 1, pp. 69-95, 2013.

[33] A. Ozawa, T. Suzuki, and I. Tanihata, "Nuclear size and related topics," *Nuclear Physics A*, vol. 693, no. 1-2, pp. 32-62, 2001.

[34] W. Nörtershäuser, D. Tiedemann, M. Žáková, Z. Andjelkovic, K. Blaum, M. L. Bissell, R. Cazan, G. W. F. Drake, Ch. Geppert, M. Kowalska, J. Krämer, A. Krieger, R. Neugart, R. Sánchez, F. Schmidt-Kaler, Z.-C. Yan, D. T. Yordanov, and C. Zimmermann, "Nuclear Charge Radii of 7,9,10Be and the One-Neutron Halo Nucleus 11Be," *Physical Review Letters*, vol. 102, no. 062503, pp. 1-4, 2009.

[35] T. Moriguchi, A. Ozawa, S. Ishimoto, Y. Abe, M. Fukuda, I. Hachiuma, Y. Ishibashi, Y. Ito, T. Kuboki, M. Lantz, D. Nagae, K. Namihira, D. Nishimura, T. Ohtsubo, H. Ooishi, T. Suda, H. Suzuki, T. Suzuki, M. Takechi, K. Tanaka, and T. Yamaguchi, "Density distributions of 11Li deduced from reaction cross-section measurements," *Physical Review C*, vol. 88, no. 024610, pp. 1-7, 2013.